STEREOVISION APPROACH FOR OBSTACLE DETECTION ON NON-PLANAR ROADS

Sergiu Nedevschi, Radu Danescu, Dan Frentiu, Tiberiu Marita, Florin Oniga, Ciprian Pocol
T.U. of Cluj-Napoca, Department of Computer Science
Email: sergiu.nedevschi@cs.utcluj.ro

Rolf Schmidt, Thorsten Graf
Volkswagen AG, Group Research, Electronics
Email: rolf4.schmidt@volkswagen.de, thorsten.graf@volkswagen.de

Keywords: Stereovision, non-flat road, road-obstacle separation, 3D points grouping, object detection, object tracking

Abstract: This paper presents a high accuracy stereovision system for obstacle detection and vehicle environment perception in various driving scenarios. The system detects obstacles of all types, even at high distance, outputting them as a list of cuboids having a position in 3D coordinates, size, speed and orientation. For increasing the robustness of the obstacle detection the non-planar road model is considered. The stereovision approach was considered to solve the road-obstacle separation problem. The vertical profile of the road is obtained by fitting a first order clothoid curve on the stereo detected 3D road surface points. The obtained vertical profile is used for a better road-obstacle separation process. By consequence the grouping of the 3D points above the road in relevant objects is enhanced, and the accuracy of their positioning in the driving environment is increased.

1 INTRODUCTION

Having a robust obstacle detection method is essential for a precise 3D environment description in driving assistance systems. The traditional approach used to detect the position, size and speed of the obstacles was the use of active sensors (radar, laser scanner). However, recent developments in computer hardware and also in image processing techniques enable the possibility of employing passive video cameras for detecting obstacles, with the advantage of a higher level of the environment description.

Obstacle detection through image processing has followed two main trends: single-camera based detection and two (or more) camera based detection (stereovision based detection). The monocular approach uses techniques such as object model fitting (Gavrila, 2000), color or texture segmentation (Ulrich, 2000), (Kalinke, 1998), symmetry axes (Kuehnle, 1998) etc. The estimation of 3D characteristics is done after the detection stage, and it is usually performed through a combination of knowledge about the objects (such as size), assumptions about the characteristics of the road (such as flat road assumption) and knowledge about the camera parameters available through calibration.

The stereovision-based approaches have the advantage of directly measuring the 3D coordinates of an image feature, this feature being anything from a point to a complex structure. The main constraints concerning stereovision applications are to minimize the calibration and stereo-matching errors in order to increase the measurements accuracy and to reduce the complexity of stereo-correlation process. The real time capability of the method is another important constraint. Such a method was proposed in (Nedevschi, 2004). The full 3D reconstruction of the visible scene is performed only on vertical or oblique edges. The list of obtained 3D points is grouped into objects based solely on density and vicinity criteria. The flat road assumption for the ground-obstacle points separation process was used. The system detects obstacles of all types, outputting them as a list of cuboids having 3D positions and sizes. The detected objects are then tracked using a multiple object-tracking algorithm, which refines the grouping and positioning, and detects the speed and orientation.

An important part in the obstacle detection process is the separation of the obstacle points from the road points. Most of the roadway obstacle detection methods are based on the flat road assumption (Weber, 1995), (Williamson, 1998). This is a poor model since deviations from the flat road may be as large as or larger than the obstacles we wish to detect. In consequence the road objects separation and the 3D objects position estimation cannot be done. Therefore the non-flat road assumption is compulsory for a robust object detection method. In literature this assumption was introduced by non-flat road approximation by series of planar surface sections (Hancock, 1997), (Labayrade, 2002) or by modeling of the non-flat roads by higher order surfaces (Goldbeck, 1999), (Aufrere, 2001). For instance the methods presented in (Aufrere, 2001), (Aufrere, 2000), (Takahashi, 1996) are fitting the parameters of a 3D clothoid model of the road lane using a monocular image and supplementary lane geometry constraints.

Our approach presented in this paper will model the vertical profile of the road surface with such a clothoid curve fitted directly on the detected 3D road surface points. These 3D road points are detected using a high accuracy stereovision method (Nedevschi, 2004). The obtained vertical profile will be used for the road-obstacle separation process in order to have a proper grouping of the 3D points in obstacles and precise estimation of their 3D position in the driving environment.

2 ENVIRONMENT MODEL

All 3D entities (points, objects) are expressed in the world coordinates system, which is depicted in figure 1.a. This coordinates system, has its origin on the ground in front of the car, the X axis is always perpendicular on the driving heading direction, the Y axes is perpendicular on the road surface and the Z axis coincides with the driving heading direction. The ego-car coordinates system has its origin in the middle of the car front axis, and the tree coordinates are parallel with the tree main axes of the car. The world coordinates system is moving along with the car and thus only a longitudinal and a vertical offset between the origins of the two coordinates system exists (vector $\mathbf{T}_{EW}$ from Figure 1). The relative orientation of the two coordinates systems ($\mathbf{R}_{EW}$ rotation matrix) will change due to static and dynamic factors. The loading of the car is a static factor. Acceleration, deceleration and steering are dynamic factors, which also cause the car to change pitch and roll angles with respect to the road surface. To obtain the pitch and roll angles and the car height we measure the distance between the car's chassis and wheels because the wheels are on the road surface. Four sensors are mounted between the chassis and wheels arms and the car height (T_X) and the pitch(R_X) and roll (R_Z) angles are computed.

Figure 1.a shows also the position of the left and the right cameras in the ego-car coordinate system. The position is completely determined by the translation vectors $\mathbf{T}_{\mathbf{CE}}^{\mathbf{i}}$ and the rotation matrices $\mathbf{R}_{\mathbf{CE}}^{\mathbf{i}}$. These parameters are essential for the stereo reconstruction process and for the epipolar line computation procedure. In order to estimate them an offline camera calibration procedure is performed after the cameras are mounted and fixed on the car using a general-purpose calibration technique. Due to the rigid mounting of the stereo system inside the car these parameters are considered to be unchangeable during driving.

The stereo reconstruction is performed in the car coordinates system. The coordinates $\mathbf{XX}_E = [X_E, Y_E, Z_E]^T$ of the reconstructed 3D points in the ego-car coordinates system can be expressed in the world coordinate system as $\mathbf{XX}_W = [X_W, Y_W, Z_W]^T$ using the following updating equation:

$$\mathbf{XX_W} = \mathbf{R}_{EW} \cdot (\mathbf{XX_E} + \mathbf{T_{EW}}) \tag{1}$$

where $\mathbf{T}_{EW}$ and $\mathbf{R}_{EW}$ are the instantaneous relative position and orientations of the two coordinates system and are computed from the damper height sensors by adding an offset to the initial value (established during camera calibration). The transformation between the rotation vector and its corresponding rotation matrix is given by the *Rodrigues* (Trucco, 1998) formulas.

$$\begin{aligned} \mathbf{T}_{EW} &= \mathbf{T}_{EW}^0 + \delta\mathbf{T}_{EW} = \mathbf{T}_{EW}^0 + [0, \delta\mathbf{T}_Y, const] \\ \mathbf{r}_{EW} &= \mathbf{r}_{EW}^0 + \delta\mathbf{r}_{EW} = \mathbf{r}_{EW}^0 + [\delta\mathbf{R}_X, 0, \delta\mathbf{R}_Z] \\ \mathbf{R}_{EW} &= Rodrigues(\mathbf{r}_{EW}) \end{aligned} \tag{2}$$

The objects are represented as cuboids, having a position (in the world coordinate system), size, orientation and velocity, as in figure 1.b. The position (X, Y, Z) and velocity ($\mathbf{v_X}$ and $\mathbf{v_Z}$) are expressed for the central lower point C of the object.

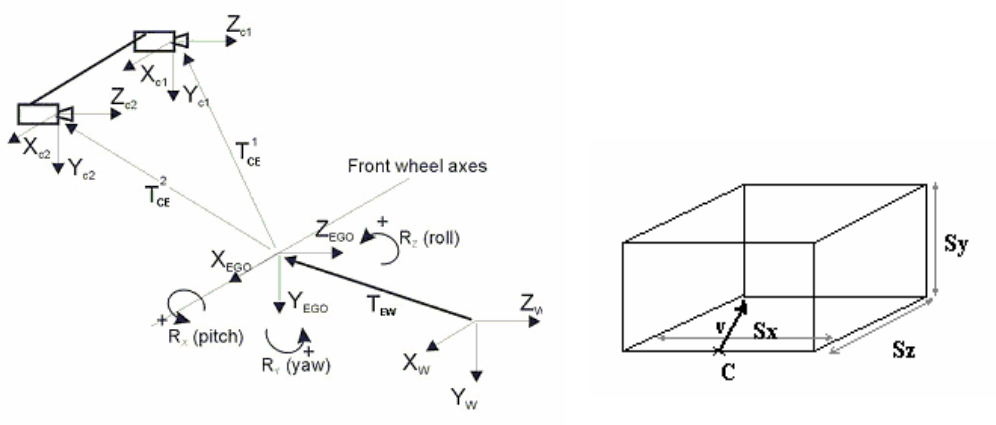

a. b.

Figure 1: a. The world, car and cameras reference systems; b. The object parameters

3 STEREO RECONSTRUCTION

The stereo reconstruction algorithm that is used is mainly based on the classical stereovision principles available in the existing literature (Trucco, 1998): find pairs of left-right correspondent points and map them into the 3D world using the stereo system geometry determined by calibration.

Constraints, concerning real-time response of the system and high confidence of the reconstructed points, must be used. In order to reduce the search space and to emphasize the structure of the objects, only edge points of the left image are correlated to the right image points. Due to the cameras horizontal disparity, a gradient-based vertical edge detector was implemented. Non-maxima suppression and hysteresis edge linking are being used. By focusing to the image edges, not only the response time is improved, but also the correlation task is easier, since these points are placed in non-uniform image areas.

Area based correlation is used. For each left edge point, the right image correspondent is searched. The sum of absolute differences (SAD) function (Williamson, 1998) is used as a measure of similarity, applied on a local neighborhood (5x5 or 7x7 pixels). Parallel processing features of the processor are used to implement this function. The search is performed along the epipolar line computed from the stereo geometry for general camera configuration.

To have a low rate of false pairs, only strong responses of the correlation function are considered as correspondents. If the global minimum of the function is not strong enough relative to other local minimums than the current left image point is not correlated. In figure 2 a successful correlation is shown along the first column, while the last two columns show ambiguous similarity functions with rejected correspondents. Repetitive patterns are rejected and only robust pairs are reconstructed.

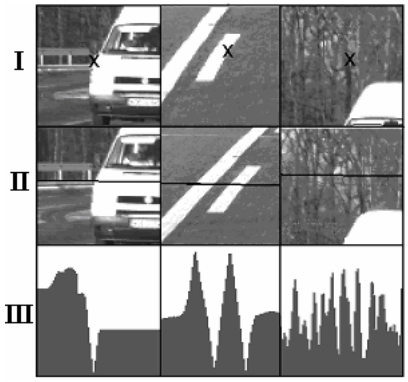

Figure 2: Three correlation scenarios are shown on each column. Left image point marked by 'x' on row I, right image search area and the epipolar line on row II and the correlation function on row III.

A parabola is fitted to a local neighborhood (3 or 5 points) of the global correlation minimum in order to detect the stereo correspondence with sub-pixel accuracy. The obtained accuracy is about 1/4 to 1/6 and is dependent of the image quality (especially noise level and contrast). Our tests proved that the 3-neighbors parabola works better than the other one.

After this step of finding correspondences, each left-right pair of points is mapped into a unique 3D point. Two 3D projection rays are traced, using the camera geometry, one for each point of the pair. By computing the intersection of the two projection rays, the coordinates of the 3D point are determined.

4 VERTICAL ROAD PROFILE ESTIMATION

Many of the obstacle detection methods assume a flat road profile. Some take into account the car pitching – therefore admitting some degree of vertical profile change – but fail to account for a possible curved vertical profile. We'll try to extract the vertical profile of the road by approximating it with a first order clothoid curve (in the ego-car coordinate system):

$$Y_E = -Z_E\alpha + c_{0,v}\frac{Z_E^{\,2}}{2} + c_{1,v}\frac{Z_E^{\,3}}{6} \qquad (3)$$

where:

α, *is* the pitch angle of the ego-car
$c_{0,y}$ – vertical curvature
$c_{1,y}$ – variation of the vertical curvature

In order to extract the coefficients α, $c_{0,v}$ and $c_{1,v}$ which will completely describe the vertical profile of the road, we'll make use of the 3D road points reconstructed by stereovision. The main advantage of using stereovision is the ability of directly extracting the vertical profile, independently of the lane detection process, sometimes even independently of the presence of any kind of delimiters. The key assumption, which makes this possible, is that there are none or very few 3D points under the road plane. Having a list of 3D points, it is easy to obtain a lateral projection in the YOZ plane, like in figure 3.

As easily can be seen, there is a lot of noise in the set of points, and therefore a simple fitting of the curve to the lower points, or a least-square clothoid fitting is not enough. Our approach to detecting the vertical profile takes two simplifying assumptions:

- In the close vicinity of the ego-vehicle (20m), the points are on a straight line, and the effect of the curvature is sensed only after the 20m interval
- The effect of roll is negligible for the vertical profile detection, that is, the vertical displacement due to roll is negligible in comparison to the displacement due to pitch and vertical curvature.

These assumptions allow us to regard the problem as a 2D curve fitting to a set of 2D points corresponding to the lateral projection of the reconstructed 3D points (figure 3).

With these assumptions, first we want to estimate the pitch angle of the ego car coordinate system relative to the road surface (angle α from equation 3). The pitch angle is extracted using a method similar to the Hough transform applied on the lateral projection of the 3D points in the near range of 0-20 m (in which we consider the road flat). Therefore, an angle histogram is built for each possible pitch angle, using the near points, and then the histogram is searched from under the road upwards. The first angle having a considerable amount of points aligned to it is taken as the pitch angle.

After detecting the pitch angle, detection of the curvature follows the same pattern. The pitch angle is considered known, and then a curvature histogram is built, for each possible curvature, but this time only the more distant 3D points (> 20 m) are taken into account, because the effect of a curvature is felt only in more distant points. The obtained vertical clothoid profile of the road is shown in figure 4.

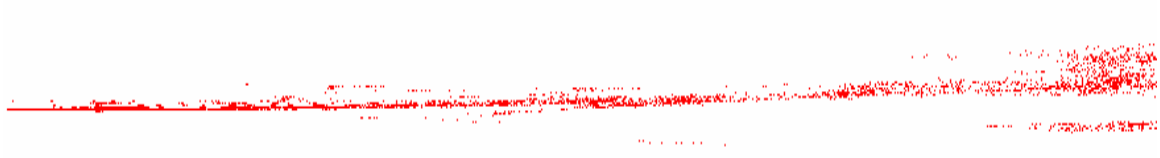

Figure 3: The 3D points in a lateral projection (YOZ plane)

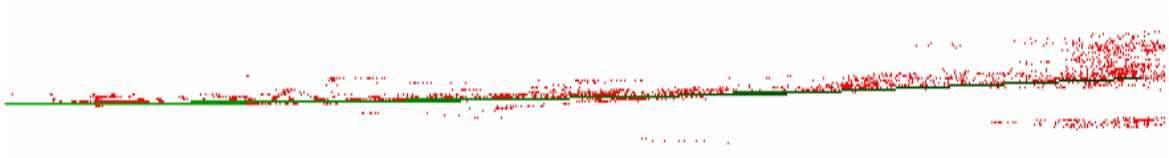

Figure 4: The vertical profile fitted to the ground points

5 GROUPING 3D POINTS INTO OBJECTS

We use only 3D points situated above the road surface. The road surface is modeled by the following clothoid equation in the world coordinates system:

$$Y = c_{0,v}\frac{Z^2}{2} + c_{1,v}\frac{Z^3}{6} \quad (4)$$

The road/obstacle separation (figure 5) of the 3D points is done using thee following constraints:

- if $|Y_W\text{-}Y| < \tau$, the point is on the road surface, and classified as road point
- if $(Y_W\text{-}Y) < -\tau$, the point is below the road, and is rejected
- if $(Y_W\text{-}Y) > \tau$, the point is above the road

The threshold τ is a positive constant and its value is chosen depending on the on the error estimation of the disparity with the depth, and on the error estimation of the clothoid parameters and possible torsion of the road.

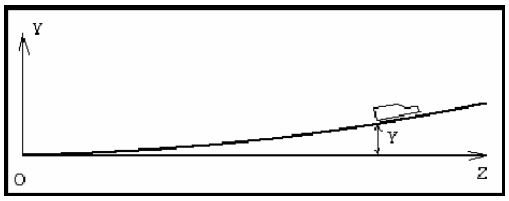

Figure 5: Lateral view of the road surface in the world coordinate system

Some supplementary constraints are used to restrict the 3D points above the road: points higher then 4m above the road surface, points that are too lateral or too far are rejected. The remaining points belong to the so-called Space of Interest (SOI) in which is performed the grouping of the 3D points in objects. For the road geometry we have made the following assumptions: in highway and most of country road scenarios the horizontal curvature is slowly changing and the torsions can be neglected in our detection range (up to 100m). Therefore knowing the road vertical profile would be enough to characterize the driving surface in the SOI.

In our SOI, no object is placed above other. Thus, on a satellite view of the 3D points in SOI, we are able to distinguish regions with high points density, representing and locating objects. Regions with low density are assumed to contain noisy points and are neglected. The satellite view (figure 6.b) of the 3D points detected from the scene depicted in figure 6.a is analyzed to identify objects.

An important observation is that the 3D points are more and more rare as the distance grows. To overcome this phenomenon, we compress the satellite view of the space (Nedevschi, 2004), depending on distance, in such a way that local density of points, in the new space, is kept constant (figure 6.c. Regardless the distance to an object, in the compressed space, the region where that object is located will have the same points density. The objects are identified as dense regions (figure 6.c). In figure 6.d the cuboids circumscribing objects are shown.

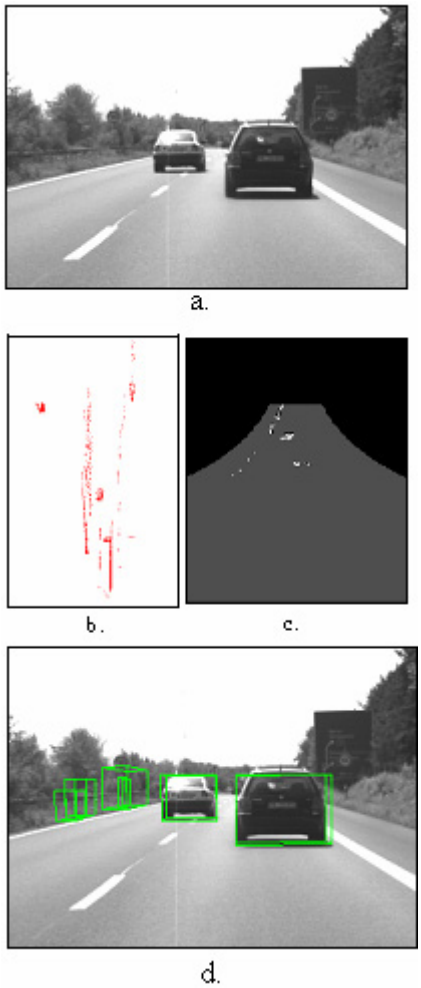

Figure 6: a. Reconstructed scene; b. Satellite view of points. c. The compressed space and the identified objects; d. Perspective view of object cuboids painted over the image

6 OBJECT TRACKING

Object tracking is used in order to obtain more stable results, and also to estimate the velocity of an object along the axes X and Z. The Y coordinate is tracked separately, using a simplified approach of simply averaging the current coordinate by the last detected coordinate.

The mathematical support of object tracking is the linear Kalman filter. The position of the object is considered to be in a uniform motion, with constant velocity. The position and speed parameters of the object along the axes X, Y and Z at the moment *k* are components of the state vector **X**(*k*) that we try to evaluate through the tracking process. The actual detection of the object will form the measurement vector **Y**(*k*), which consists only of the coordinates of the detected object.

$$\mathbf{X}(k) = \begin{bmatrix} x(k) & y(k) & z(k) & v_x(k) & v_Y(k) & v_z(k) \end{bmatrix}^T \quad (5)$$

The evolution of the **X** vector is expressed by the linear equation:

$$\mathbf{X}(k) = \mathbf{A}(k) \times \mathbf{X}(k-1) \quad (6)$$

where the state transition matrix **A**(*k*) is

$$\mathbf{A} = \begin{bmatrix} 1 & 0 & 0 & \Delta t & 0 & 0 \\ 0 & 1 & 0 & 0 & \Delta t & 0 \\ 0 & 0 & 1 & 0 & 0 & \Delta t \\ 0 & 0 & 0 & 1 & 0 & 0 \\ 0 & 0 & 0 & 0 & 1 & 0 \\ 0 & 0 & 0 & 0 & 0 & 1 \end{bmatrix} \quad (7)$$

The steps of tracking a single object are:

Prediction: a new position of the object is computed using the last state vector and the transition matrix, through equation (6).

Measurement: around the predicted position (*pX ,pY, pZ*) we search for objects resulted from grouping which have the distance to the prediction below a threshold. The distance is computed by equation (8), which gives different weights to displacements along the three coordinate axes, and take into consideration also the current object speed, which is seen as an indetermination factor.

$$D(x,y,z) = 2\left|\,|x - pX| - \left|\frac{v_x}{3}\right|\,\right| + 0.7|y - pY| + 0.5\left|\,|z - pZ| - \left|\frac{v_z}{3}\right|\,\right| \quad (8)$$

The objects that satisfy the vicinity condition are used to form an envelope whose position is computed and used as measurement, and the size of the envelope is used as the current measurement of the tracked object's size. By creating an envelope object out of the objects near a track we can join objects that were previously detected as separate. This merging becomes effective only if the separated objects have the same trajectory. This is ensured by the object-track association, when track compete for objects, and a false object joining won't last for too long.

Update: The measurement and the prediction are used to update the state vector **X** through the equations of the Kalman filter. The Y coordinate and the object's size are tracked by averaging the current measurement with the past measurements. If in the current frame there is no measurement that can be associated to the track, the prediction is used as output of the tracking system. The track is considered lost after a number of frames without measurement.

Tracking multiple objects adds a little bit more complexity to the algorithm presented above. We have to decide which detected object belongs to which track, or if a detected object starts a new track. The association between detected objects and tracks is done using a modified nearest-neighbor method, using the distance expressed by equation (8). Each object is compared against each track. The objects are labeled employing the nearest track identity number, provided that there is at least one track that has a sufficient low distance to the object. The modification from the classical nearest-neighbor scheme is that we introduce an "age discount" in the distance comparison, and in this way we give priority to the older, more established tracks. This discounting mechanism is achieved by sorting the tracks in the reverse order of their age (the older ones first). If we compare an object to a track and the object already was labeled with the label of another track, we change the owner of the object only if the distance object-current track is lower than the distance to the older track minus a fixed quantity, the age discount.

For every object that cannot be assigned to an existing track and that fulfills some specific conditions, a new track is initialized. A new track is

started for a single object that has a reasonable size. There is no object joining in the initialization phase of a track. In this way we avoid initializing tracks to noise objects, and thus amplifying the noise. Tracks are aborted if the association process fails for a predefined number of frames. A tracking validation process based on the image of the object is employed in order to ensure that there is no track switching from one object to another.

7 RESULTS

The detection system has been deployed on a standard 1 GHz Pentium® III personal computer, and the whole processing cycle takes less than 100 ms processing time, therefore securing a 10 fps detection rate. This makes the system suitable for real-time applications. The system has been tested in various traffic scenarios, both offline (using stored sequences) and online (on-board processing), and acted well in both conditions. In all situations the obstacles were reliably detected and tracked, and their position, size and velocity measured. The detection has proven to have a maximum working range of about 90 m, with maximum of reliability in the range 10-60 m. The depth measurement error is, naturally, higher than one can obtain from a radar system, but it is very low for a vision system: less than 10 cm of error at 10 m, about 30 cm of error at 45 m and about 2 m of error at 95 m.

In figure 7 the detection results on a non-flat road are outlined. The scene from figure 6.a is at the end of a concave slope. The detected road surface has a concave vertical curvature $c_{0,v} \approx 2e^{-4}$. The far objects (the two cars at 71m, respectively 81m and the traffic sign from 91m have vertical offsets in the world coordinates system (having the XOZ plane coincident with the road surface below the current car position) of 0.51m, 0.66m and 0.96m respectively, due to the non flat road. But using the non-flat road modeled by a vertical clothoid (figure 6.b) the objects are detected correctly on the road surface.

8 CONCLUSIONS

We have presented a stereovision-based obstacle detection system that reconstructs and works on 3D points corresponding to the object edges, in a large variety of traffic scenarios, and under real-time constraints. Because the stereovision module reconstructs any feature in sight (that means also the road features) the vertical profile of the road was detected. This way a correct road-obstacle separation was possible. The grouping of the 3D points in relevant objects was greatly improved, and the objects 3D positioning accuracy was increased.

The functions of this system can be greatly extended in the future. An intelligent correlation function should be developed, one that can disambiguate, not reject, repetitive patterns and reconstruct points from horizontal edges. Moreover, because any type of object is detected this algorithm can form the basis for any type of specific object detection system, such as vehicle detection, pedestrian detection, or even traffic sign detection. The classification routines can be performed directly on our detected objects, with the advantage of reduced search space and additional helpful information such as distance, size and speed, which can also reduce the class hypotheses. The vertical road profile detection from stereovision can be the base for a 3D lane detection algorithm, which will give a complete 3D description of the driving environment in a lane related coordinates system.

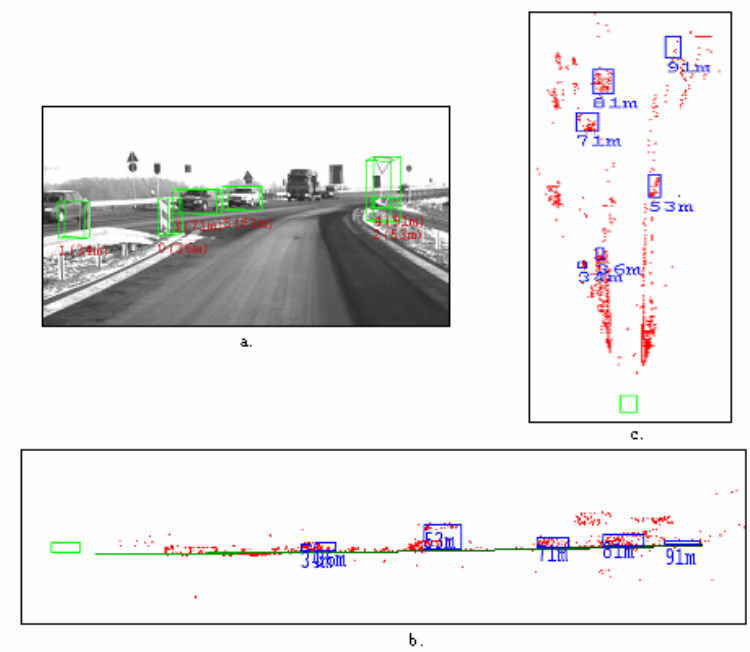

Figure 7: a. Image of the scene with the detected object (cuboids with ID and distance); b. Side view of the detected objects and the detected road surface; c. Top view of the detected objects.

REFERENCES

Gavrila, D. M, 2000. Pedestrian Detection from a Moving Vehicle. In Proc. of European Conference on Computer Vision, Dublin, Ireland, 2000, pp. 37-49

Ulrich, I, Nourbakhsh, I, 2000. Appearance-Based Obstacle Detection with Monocular Color Vision. In Proc. of the AAAI National Conference on Artificial Intelligence, Austin, TX.

Kalinke, T, Tzomakas, C, von Seelen, W, 1998. A Texture based Object Detection and an Adaptive Model-based Classification. In Procs. IEEE Intelligent Vehicles Symposium'98, (Stuttgart, Germany), pp. 341–346.

Kuehnle, A, 1998. Symmetry-based vehicle location for AHS. In Procs. SPIE Transportation Sensors and Controls: Collision Avoidance, Traffic Management, and ITS, vol. 2902, (Orlando, FL), pp. 19–27.

Nedevschi, S, Schmidt, R., Graf, T, Danescu, R, Frentiu, D, Marita, T, Oniga, F, Pocol, C, 2004. High Accuracy Stereo Vision System for Far Distance Obstacle Detection. In IEEE Intelligent Vehicles Symposium '04, Parma, Italy.

Weber, J, Koller, T, Luong, Q.-T, Malik, J, 1995. An integrated stereo-based approach to automatic vehicle guidance. In Fifth International Conference on Computer Vision, In Collision Avoidance and Automated Traffic Management Sensors, Proc. SPIE 2592.

Williamson, T. A, 1998. A high-performance stereo vision system for obstacle detection. PhD Thesis CMU-RI-TR-98-24, Robotics Institute Carnegie Mellon University, Pittsburg, September.

Hancock, J, 1997. High-Speed Obstacle Detection for Automated Highway Applications. Tech. Report CMU-RI-TR-97-17, Robotics Institute, Carnegie Mellon University, Pittsburg.

Labayrade, R, Aubert, D, Tarel, J P, 2002. Real Time Obstacle Detection in Stereovision on Non Flat Road Geometry Through V-disparity Representation. In Proceedings of IEEE Intelligent Vehicle Symposium, IV '02), Versailles, France.

Goldbeck, J, Huertgen, B, 1999. Lane Detection and Tracking by Video Sensors. In IEEE International Conference on Intelligent Transportation Systems (ITSC 99).

Aufrere, R, Chapuis, R, Chausse, F, 2001. A model-driven approach for real-time road recognition. In Machine Vision and Applications, Springer-Verlag.

Aufrere, R, Chapuis, R, Chausse, F, 2000. A fast and robust vision-based road following algorithm. In IEEE-Intelligent Vehicles Symposium 2000, pp.192-197.

Takahashi, A, Ninomiya, Y, 1996. Model-based lane recognition. In Proceedings of the IEEE Intelligent Vehicles Symposium 1996, pp. 201–206.

Trucco, E, Verri, A, 1998. *Introductory Techniques for 3D Computer Vision.* Prentice-Hall, New Jersey.